Diagn Interv Radiol 2020; 26:264–270

ABDOMINAL IMAGING

ORIGINAL ARTICLE

Influence of tube voltage, tube current and newer iterative reconstruction algorithms in CT perfusion imaging in rabbit liver VX2 tumors

Jing-Lei Li*
Wei-Tao Ye*
Li-Fen Yan
Zai-Yi Liu
Xi-Ming Cao
Chang-hong Liang

PURPOSE
We aimed to explore the influence of tube voltage, current and iterative reconstruction (IR) in computed tomography perfusion imaging (CTPI) and to compare CTPI parameters with microvessel density (MVD).

METHODS
Hepatic CTPI with three CTPI protocols (protocol A, tube voltage/current 80 kV/40 mAs; protocol B, tube voltage/current 80 kV/80 mAs; protocol C: tube voltage/current 100 kV/80 mAs) were performed in 25 rabbit liver VX2 tumor models, and filtered back projection (FBP) and IR were used for reconstruction of raw data. Hepatic arterial perfusion (HAP), hepatic portal perfusion (HPP), total perfusion (TP), hepatic arterial perfusion index (HPI), blood flow (BF) and blood volume (BV) of VX2 tumor and normal hepatic parenchyma were measured. Image noise, signal-to-noise ratio (SNR) and contrast-to-noise ratio (CNR) were quantified and radiation dose was recorded. MVD was counted using CD34 stain and compared with CTPI parameters.

RESULTS
The highest radiation dose was found in protocol C, followed by protocols B and A. IR lowered image noise and improved SNR and CNR in all three protocols. There was no statistical difference between HAP, HPP, TP, HPI, BF and BV of VX2 tumor and normal hepatic parenchyma among the three protocols ($P > 0.05$) with FBP or IR reconstruction, and no statistical difference between IR and FBP reconstruction ($P > 0.05$) in either protocol. MVD had a positive linear correlation with HAP, TP, BF, with best correlation observed with HAP; MVD of VX2 tumor showed no or poor correlation with HPI and BV.

CONCLUSION
CTPI parameters are not affected by tube voltage, current or reconstruction algorithm; HAP can best reflect MVD, but no correlation exists between BV and MVD.

Global cancer statistics 2018 reports that liver cancer is the sixth most commonly diagnosed cancer and fourth leading cause of cancer death (1), and it is particularly common in China. There are several treatments for liver cancer, including surgery, targeted therapy, transcatheter arterial chemoembolization, radiofrequency ablation, conventional chemical therapy, and others (2). Surgery is the first choice with limited clinical indications, because most hepatic tumors are in advanced stage at first detection. Modern imaging modalities play a key role not only in accurately making preoperative evaluation to guide optimal treatment, but also in assessing response to treatment to determine further treatment and prognosis for patients with advanced hepatic malignances.

At present, ultrasonography, computed tomography (CT) and magnetic resonance imaging (MRI) are commonly chosen for the diagnosis and monitoring of hepatic malignancies by response evaluation criteria in solid tumors (RECIST) (3) or modified RECIST (4) to evaluate the change in size of hepatic tumors for guiding further treatment. However, there may be response to treatment, but no change in size for those receiving nonsurgical treatment. Accurate evaluation of treatment response and detection of ineffective treatment in early stages may affect further management. Therefore, it is imperative to develop new imaging standards to better display the characteristic biological effect of treatment on the hepatic tumor.

From the Departments of Radiology (J.L.L ✉ *lijinglei80@126.com*, W.T.Y., L.F.Y., Z.Y.L., X.M.C., C.H.L ✉ *cjr.lchh@vip.163.com*) Guangdong General Hospital, Guangdong Academy of Medical Sciences, Guangzhou, China.

*Jing-Lei Li and Wei-Tao Ye contributed equally to this work.

Received 24 March 2019; revision requested 06 May 2019; last revision received 21 October 2019; accepted 03 November 2019.

Published online 27 May 2020.

DOI 10.5152/dir.2019.19147

You may cite this article as: Li JL, Ye WT, Yan LF, Liu ZY, Cao XM, Liang CH. Influence of tube voltage, tube current and newer iterative reconstruction algorithms in CT perfusion imaging in rabbit liver VX2 tumors. Diagn Interv Radiol 2020; 26:264–270.

Perfusion imaging modalities, including dynamic contrast-enhanced MRI (DCE-MRI) and computed tomography perfusion imaging (CTPI), show tremendous prospects. DCE-MRI is used for evaluation of tissue perfusion and permeability by determining arterial flow, portal flow, arterial fraction, mean transit time, and distribution volume of gadolinium contrast media with a pharmacokinetic model (5). DCE-MRI has the advantage of repeated inspection with no radiation, but it is greatly affected by respiratory movement and long scanning times with poor repeatability and accuracy, and it is limited in wide application due to higher technological requirements. As a noninvasive functional imaging method, CTPI can supply the information of microcirculatory perfusion by implementing continuous dynamic scanning. It was previously reported that the quantitative parameters of hepatic CTPI were highly accurate, repeatable, and consistent (6–8), and showed significant correlation with the presence and degree of tumor vessels (9–11). Therefore, CTPI can be valuably used to detect hepatic tumors early on, individually monitor therapeutic effect, and assess prognosis more accurately than morphological imaging technologies (12). However, the disadvantage of high radiation dose has limited the widespread use of CTPI, especially for patients with advanced hepatic malignancy, who should have repeated inspections to monitor response to treatment. Besides, due to lack of standardization and unified protocol for CTPI scanning, the radiation dosage varies tremendously from 7.3 to 30.6 mSv (13). It is necessary to reduce radiation dose for further improving the feasibility of hepatic CTPI and promoting its clinical application. There are two ways to reduce radiation dose, including optimizing scanning parameters (e.g., tube voltage and tube current) and using newer or recent image reconstruction algorithms (e.g., iterative reconstruction, IR) (14).

Main points

- Computed tomography perfusion imaging (CTPI) plays a key role not only in accurate preoperative evaluation to guide optimal treatment, but also in assessing response to treatment to determine further treatment and prognosis for patients with advanced hepatic malignances.
- It is necessary to reduce the radiation dose for improving the feasibility of hepatic CTPI and promoting its clinical application.
- CTPI parameters are not affected by tube voltage, current, or reconstruction algorithms; hepatic arterial perfusion can best reflect microvessel density (MVD), but there is no correlation between blood volume and MVD.

The principal aim of the study is to investigate the influence of tube voltage, tube current and IR in hepatic CTPI parameters and to study the correlation between CTPI parameters and histopathological microvessel density (MVD) in the rabbit liver VX2 tumor model.

Methods

The local institutional animal care and use committee approved this study (No. GDREC2014012A).

Experimental animal models

Thirty New Zealand white rabbits (weight 2000–3000 g, 5–6 months, no gender restriction; from Xingke animal farm of Guangzhou) were used in this study. All animal models were made and raised with supervision of GB14922-94 standard (Animal experiment center of Southern Medical University, Guangzhou). After IV injection of pentobarbital sodium (3%, 1 mL/kg) for successful anesthetization, liver was exposed and VX2 tumor tissue suspension (0.2–0.3 mL) was locally injected into hepatic parenchyma with a 1 mL syringe. The incision was carefully stitched after hepatic injection point bleeding ceased.

After 3–4 weeks of implantation, ultrasonography was performed to confirm tumor's location and size, then unenhanced CT was performed for VX2 models with tumors of 1–3 cm in size. Based on unenhanced CT findings, intrahepatic single tumors of 1–3 cm and no prominent necrosis were included in the experimental group, but multiple tumors, or tumors >3 cm in size or obvious necrosis or extrahepatic tumors were excluded.

Hepatic CTPI protocols and postprocess images

After anesthesia by injecting 20% urethane into abdominal cavity (10 mL + additional 5 mL at a time, based on the condition of anesthesia), the animals were fixed in supine position with free breathing. A 256-slice Brilliance iCT scanner (Philips Healthcare) was used for imaging. Unenhanced CT scan was performed to determine scanning coverage with fixed tube voltage 120 kV and fixed current 80 mAs; other parameters included slice thickness 2.5 mm, pitch 0.99, collimation 128×0.625, field of view 136 mm, matrix 512×512, standard focal spot resolution, Iohexol 350 mgI/mL (5 mL) + saline (5 mL) was injected intravenously at 1.0 mL/s for 1.5 s using a double tube high-pressure syringe (Ulrich medical). Hepatic CTPI with stationary axial scan model (NON-JOG) was repeated 40 times with 0.58 s scan time, 1.5 s interval time. Three CTPI protocols (protocol A: tube voltage 80 kV, tube current 40 mAs; protocol B: tube voltage 80 kV, tube current 80 mAs; protocol C: tube voltage 100 kV, tube current 80 mAs) were randomly repeated for each animal model. The interval time was at least 1 hour between first and second CTPI scans, at least 2 hours between second and third scans. The entire VX2 tumor and partial spleen was covered with fixed scan length of 40 mm. Other parameters were the same as those of unenhanced CT scans.

The raw data was reconstructed by IR (iDose4 Level3) and filtered back projection (FBP), then analysis was conducted with functional CT software package (general perfusion and liver perfusion types) on an external BrillianceTM Workspace 4.0.2.144 (Philips). Region of interest (ROI) was drawn respectively within aorta of 12th thoracic vertebral level as input artery, main portal vein as input vein, and the most significant enhanced area of the spleen. Time density curve was generated automatically by using maximum slope method to obtain perfusion parameters, which included hepatic arterial perfusion (HAP), hepatic portal perfusion (HPP), total perfusion (TP), hepatic arterial perfusion index (HPI), blood flow (BF) and blood volume (BV). ROI was drawn on three consecutive maximum images of VX2 tumor, as well as on normal hepatic parenchyma at the same slices (Fig.), and the average values were calculated as perfusion values. ROI for VX2 tumor was drawn as large as possible, avoiding prominent vessels, obvious necrosis, and adjacent normal parenchyma. ROI for normal hepatic parenchyma was 0.5–3.0 cm^2 (as large as possible) and placed at normal hepatic subcapsular parenchyma of left and right lobes, avoiding obvious vessels and artifact. The average values were calculated as perfusion values. ROI with similar shape and size were placed at the same level and same site on FBP and IR images of the same scan, and at the similar level and site on three CTPI protocol images of the same model. Two in-

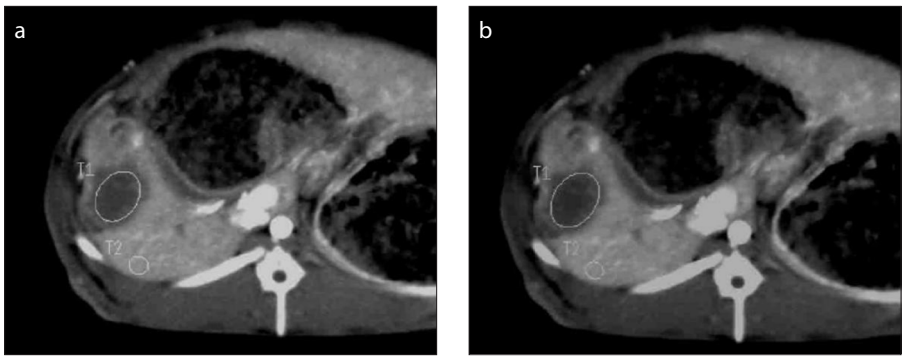

Figure. a, b. A rabbit model with liver VX2 tumor located in the right lobe. Region of interest (ROI) in VX2 tumor (T1) and normal hepatic parenchyma should keep the same shape and size in both filtered back projection **(a)** and iterative reconstruction **(b)** images of the same CT perfusion imaging. The ROI should be as large as possible, covering most of VX2 tumor, and omitting adjacent normal parenchyma, obvious vessels and prominent necrosis.

dependent radiologists measured the above perfusion parameters.

CT value and image noise of VX2 tumor and background tissue (erector spinae) were measured with similar ROI on the same three consecutive images mentioned above, and signal-to-noise ratio (SNR) and contrast-to-noise ratio (CNR) were derived.

Radiation dose parameters of each CTPI scan of all animal models were obtained, including volume CT dose index (CTDIvol) in mGy, dose-length product (DLP) in mGy cm and effective dose (ED) in mSv. The calculation of effective dose was made by multiplying DLP with conversion coefficient (k=0.015 mSv/mGy cm).

Histological analysis

All animal models were sacrificed by intravenously injecting an overdose of 20% urethane and VX2 tumor specimens were fixed in 20% neutral buffered formalin. The histological features were evaluated by hematoxylin-eosin (H-E) staining. The microvessel density (MVD) was quantified on CD34 stained sections by manually measuring the number of microvessels at high magnification (×400), in five random fields-of-view with high microvessel intensity, and the average MVD value was calculated.

Statistical analysis

All statistical analyses were performed using SPSS 19.0 statistical package (SPSS Inc.). Raw data were summarized using mean ± standard deviation. A *P* value of <0.05 was considered as statistically significant. Reliability analysis was used to determine the observers' agreement in measurement of each CTPI parameter. Repeated measurement data with linear mixed models (LMMs) and Mann-Whitney U test were used to analyze the difference of non-contrast CT value, CTPI parameters, radiation dose and objective image quality among three CPTI scan protocols. Paired-sample *t* test or Wilcoxon paired-sample test was used to compare the difference of objective image quality and CTPI parameters between FBP and IR-iDose4 Level3. The correlations between CTPI parameters and MVD were quantified with Pearson correlations (r), with r ≥0.7 indicating a good correlation; r, 0.4–0.7 a fair correlation; r <0.4 a poor correlation.

Results

Hepatic VX2 tumor models were successfully established in 25 rabbits, showing single low density lesion, which located in the left and right lobes in 18 and 7 cases, respectively. CTPI of protocol A, B, and C were performed in 23, 22, and 23 cases, respectively. Three rabbits died accidentally during raising, one rabbit due to anesthesia accident, and one rabbit model with extrahepatic VX2 tumor was excluded.

The radiation dose of CTPI was highest with protocol C (DLP, 2382.81±1.59 mGy•cm; ED, 35.74±0.02 mSv), followed by protocol B (DLP, 1273.86±1.15 mGy•cm; ED, 19.11±0.18 mSv) and protocol A (DLP, 632.81±1.07 mGy•cm; ED, 9.49±0.16 mSv) with statistically significant difference among all three CTPI protocols (repeated measurement data with LMMs: DLP, F=9244245, $P < 0.001$; ED, F=8660468, $P < 0.001$) and between each pair of CTPI protocols (Mann-Whitney U test: $P < 0.001$, for all).

The average CT value, image noise, SNR and CNR of VX2 tumors of three CTPI protocols combined with FBP and IR were listed in Table 1.

Independent of reconstruction algorithm, CT value and image noise of VX2 tumor of protocol C was significantly lower than that of protocols A and B ($P < 0.05$), but no statistical difference was found between protocols A and B ($P > 0.05$). For each CTPI protocol, FBP of VX2 tumor yielded significantly higher CT values than those with IR (paired-sample *t* test: $P < 0.05$). Image noise of VX2 tumor was significantly higher with FBP than with IR using protocols A and B ($P < 0.05$), but no statistical difference was seen with protocol C ($P > 0.05$).

Independent of FBP or IR, SNR and CNR of VX2 tumor did not differ significantly among the three protocols (repeated measurement data with LMMs: $P > 0.05$). SNR of VX2 tumor was lower with FBP than with IR, with statistically significant difference for protocol B (paired-sample *t* test: $P < 0.05$), while the difference was not statistically significant for protocols A and C. For each CTPI protocol, CNR of VX2 tumor was slightly higher with IR than that with FBP, but the difference was not statistically significant (Wilcoxon paired-sample test, $P > 0.05$).

There was good or excellent reproducibility of HAP, HPI, TP, HPI, BF, and BV between the two observers (intraclass correlation coefficients [ICCs] for VX2 tumor: 0.680–0.820 with IR, 0.667–0.863 with FBP; ICCs for normal hepatic parenchyma: 0.797–0.927 with IR, 0.633–0.969 with FBP).

Independent of FBP or IR, HAP, HPP, TP, HPI, BF and BV of VX2 tumor and normal hepatic parenchyma were not significantly different among the three CTPI protocols (repeated measurement data with LMMs: $P > 0.05$). Independent of CTPI protocols, HAP, HPP, TP, HPI, BF and BV of VX2 tumor and normal hepatic parenchyma were not significantly different between IR and FBP (paired-sample *t* test: $P > 0.05$). CTPI parameters of VX2 tumors and normal hepatic parenchyma of three CTPI protocols combined with FBP and IR were detailed in Tables 2 and 3, respectively.

Independent of reconstruction algorithm or CTPI protocol, MVD of VX2 tumor had a positive linear correlation with HAP, TP, BF, with best correlation observed with HAP; MVD of VX2 tumor showed no or poor correlation with HPI and BV. Pearson correlation coefficients between MVD and CTPI parameters of the three protocols combined with IR or FBP were detailed in Table 4.

Table 1. Objective image quality of liver VX2 tumors of three CTPI protocols combined with FBP and IR

Parameters	Algorithm	Protocol A (n=23)	Protocol B (n=22)	Protocol C (n=23)	*F*	*P*
CT value	IR	102.88±17.44	97.23±13.10	85.56±7.80	11.184	<0.001
	FBP	106.97±17.48	100.94±13.24	87.51±7.71	14.651	<0.001
	t	8.468	9.182	13.264		
	P	<0.001	<0.001	<0.001		
Image noise	IR	10.56±2.66	10.11±2.40	8.40±2.09	8.131	0.001
	FBP	11.37±2.66	11.12±2.66	8.56±1.67	14.845	<0.001
	t	2.715	3.813	0.626		
	P	0.013	0.001	0.538		
SNR	IR	10.22±2.23	10.32±3.01	10.87±2.79	0.457	0.636
	FBP	9.82±1.95	9.74±2.56	10.68±2.20	1.343	0.272
	t	1.537	2.525	0.634		
	P	0.140	0.020	0.533		
CNR	IR	2.24±1.52	2.01±1.24	1.68±1.37	0.866	0.426
	FBP	2.06±1.40	1.94±1.00	1.63±1.24	0.712	0.495
	Z	1.651	0.643	1.269		
	P	0.099	0.520	0.205		

Data are presented as mean ± standard deviation.
CTPI, computed tomography perfusion imaging; CT, computed tomography; IR, iterative reconstruction (iDose4 Level3); FBP, filtered back projection; SNR, signal-to-noise ratio; CNR, contrast-to-noise ratio.

Table 2. CTPI parameters of liver VX2 tumors of three different CTPI protocols combined with FBP and IR

Parameters	Algorithm	Protocol A (n=23)	Protocol B (n=22)	Protocol C (n=23)	*F*	*P*
HAP	IR	17.09±11.90	17.59±9.28	16.75±8.75	0.170	0.844
	FBP	17.16±12.89	17.98±9.79	16.59±8.06	0.229	0.796
	t	0.168	1.091	0.424		
	P	0.868	0.288	0.676		
HPP	IR	11.20±8.46	9.19±5.53	8.71±4.14	1.519	0.230
	FBP	10.62±7.75	10.87±8.89	8.22±3.46	1.290	0.285
	t	0.892	1.332	0.617		
	P	0.382	0.197	0.543		
TP	IR	28.28±18.69	26.78±12.31	25.46±10.36	1.090	0.345
	FBP	27.77±19.16	28.85±16.56	24.81±9.44	0.948	0.396
	t	0.791	1.402	0.709		
	P	0.437	0.176	0.486		
HPI (%)	IR	60.80±11.07	65.17±12.19	64.44±12.66	0.842	0.438
	FBP	60.87±11.45	63.88±12.43	65.98±10.27	1.224	0.304
	t	0.036	0.812	1.282		
	P	0.972	0.426	0.213		
BF	IR	6.21±6.31	5.28±3.09	6.70±4.67	1.587	0.216
	FBP	6.05±5.83	5.77±4.34	6.37±4.42	0.317	0.730
	t	0.243	1.365	0.824		
	P	0.811	0.187	0.419		
BV	IR	10.01±6.59	10.12±4.35	9.66±3.53	0.077	0.926
	FBP	11.16±9.34	9.54±4.41	9.75±3.56	0.673	0.515
	t	1.336	2.011	0.538		
	P	0.195	0.057	0.596		

Data are presented as mean ± standard deviation.
CTPI, computed tomography perfusion imaging; IR, iterative reconstruction (iDose4 Level3); FBP, filtered back projection; HAP, hepatic arterial perfusion (mL/min/100 mg); HPP, hepatic portal perfusion (mL/min/100 mg); TP, total perfusion (mL/min/100 mg); HPI, hepatic arterial perfusion index (%); BF, blood flow (mL/min/100 mg); BV, blood volume (mL/100 mg).

Table 3. CTPI parameters of normal hepatic parenchyma of three different CTPI protocols combined with FBP and IR

Parameters	Algorithm	Protocol A (n=23)	Protocol B (n=22)	Protocol C (n=23)	*F*	*P*
HAP	IR	35.62±13.19	39.31±18.01	37.20±12.07	0.091	0.913
	FBP	38.20±13.32	37.24±18.36	36.41±10.31	0.590	0.559
	t	1.635	2.070	0.794		
	P	0.116	0.051	0.436		
HPP	IR	120.08±46.88	124.99±46.88	104.02±35.68	1.564	0.222
	FBP	117.37±42.25	123.27±57.11	100.61±38.07	1.647	0.205
	t	0.558	0.344	1.026		
	P	0.582	0.734	0.317		
TP	IR	155.70±53.35	164.29±45.74	141.22±40.06	1.778	0.182
	FBP	155.57±47.99	160.51±51.00	137.03±41.92	1.818	0.175
	t	0.025	0.729	0.709		
	P	0.980	0.474	0.486		
HPI	IR	24.43±8.52	26.48±15.34	28.22±7.81	0.824	0.446
	FBP	25.89±9.67	25.61±15.79	29.42±9.90	1.034	0.364
	t	0.975	0.862	1.282		
	P	0.340	0.398	0.213		
BF	IR	44.84±15.71	48.39±9.53	42.42±10.27	0.845	0.437
	FBP	46.22±15.60	48.48±12.44	42.07±9.64	1.974	0.152
	t	1.930	0.074	0.824		
	P	0.067	0.942	0.419		
BV	IR	30.54±7.49	32.86±10.27	29.79±6.30	0.910	0.410
	FBP	29.85±6.81	31.26±9.45	30.70±6.74	0.247	0.782
	t	0.693	2.095	1.485		
	P	0.495	0.048	0.152		

Data are presented as mean ± standard deviation.
CTPI, computed tomography perfusion imaging; IR, iterative reconstruction (iDose4 Level3); FBP, filtered back projection; HAP, hepatic arterial perfusion (mL/min/100 mg); HPP, hepatic portal perfusion (mL/min/100 mg); TP, total perfusion (mL/min/100 mg); HPI, hepatic arterial perfusion index (%); BF, blood flow (mL/min/100 mg); BV, blood volume (mL/100 mg).

Discussion

According to as low as reasonably achievable (ALARA) principle (15), CTPI radiation should be decreased to the minimum level while sufficient image quality is maintained for reliable diagnosis, which is a tremendous challenge. Previous studies have shown that when lowering tube voltage and/or tube current to decrease radiation, the imaging quality will definitely decrease; however, compared with conventional FBP, IR is able to selectively eliminate image noise and maintain or improve imaging quality (16–20). Our study compared the influence of different tube voltages, tube currents and reconstruction algorithms in hepatic CTPI and imaging quality in 256-slice MDCT, which had not been systemically studied in the past.

Our study reconfirms that radiation dose can be effectively decreased by decreasing tube voltage and tube current. There was a linear relationship between radiation dose and tube current at fixed voltage setting: compared with protocol B, tube current was 50% less in protocol A, which resulted in about 50% decrease in the radiation dose. On the other hand, lowering the tube voltage at fixed tube current allowed for a sharper decline in the radiation dose, which was proportional to the square of tube voltage: compared with protocol C, tube voltage was 20% less in protocol B, which resulted in 46.54% decrease in the radiation dose. But overall, the increase of image noise and decrease of SNR and CNR was not significant, and the radiation dose of protocol A was still too high at about 9.48 mSv, mainly due to the small size of the animal, relatively higher scanning parameters, and too many continuous scanning times for more accurate perfusion parameters. In other words, tube voltage, tube current, and scanning times can be further decreased, and the exact adjustments need to be verified in the clinical setting in future. Furthermore, our study also reconfirmed that IR has the ability to decease image noise and improve image quality of both VX2 tumor and normal hepatic parenchyma, similar to previous reports (16–20).

Consistent with previous studies (6, 21), the reproducibility of CTPI parameters was excellent. CTPI parameters of both VX2 tumors and normal hepatic parenchyma were not significantly different between different reconstruction algorithms and among different scanning protocols in our study, similar to previous studies (22, 23). Therefore, it can be inferred that reconstruction algorithm, tube current, and tube voltage

Table 4. Pearson correlation coefficient between MVD and CTPI parameters of three protocols combined with IR or FBP reconstruction

		IR vs. MVD		FBP vs. MVD	
Protocols	Parameters	r	*P*	r	*P*
Protocol A	HAP	0.809	<0.001	0.810	<0.001
	HPP	0.626	0.001	0.623	0.001
	TP	0.798	<0.001	0.797	<0.001
	HPI	0.116	0.599	0.271	0.212
	BF	0.771	<0.001	0.665	0.001
	BV	0.493	0.017	0.543	0.007
Protocol B	HAP	0.804	<0.001	0.803	<0.001
	HPP	0.260	0.243	0.413	0.056
	TP	0.722	<0.001	0.696	<0.001
	HPI	0.456	0.033	0.246	0.269
	BF	0.624	0.002	0.584	0.004
	BV	0.170	0.450	0.215	0.336
Protocol C	HAP	0.594	0.003	0.633	0.001
	HPP	0.158	0.472	0.095	0.667
	TP	0.566	0.005	0.506	0.014
	HPI	0.435	0.038	0.607	0.002
	BF	0.757	<0.001	0.869	<0.001
	BV	0.503	0.014	0.564	0.005

MVD, microvessel density; CTPI, computed tomography perfusion imaging; IR, iterative reconstruction (iDose4 Level3); FBP, filtered back projection; HAP, hepatic arterial perfusion (mL/min/100 mg); HPP, hepatic portal perfusion (mL/min/100 mg); TP, total perfusion (mL/min/100 mg); HPI, hepatic arterial perfusion index (%); BF, blood flow (mL/min/100 mg); BV, blood volume (mL/100 mg).

has no influence in CTPI parameters, mainly because CTPI parameters are calculated by time-density curve (TDC); the shape of TDC and derived-parameters do not change with varying CT values caused by the adjustment of scanning parameters or reconstruction algorithm, but only depending on the blood perfusion. Our results provide an experimental basis for further lowering radiation dose of CTPI, but further validation in clinic is needed in future studies.

Although accepted as the gold standard for evaluation of tumor angiogenesis, MVD is limited by invasive biopsy and in reflecting the overall blood supply of tumor *in vivo*, which only represents localized angiogenesis but not the whole tumor. CTPI is a noninvasive technique to evaluate angiogenesis and blood supply of whole tumors *in vivo*. However, there are still some controversies about correlation between CTPI parameters and pathological features of neovascularization in tumors. Our study showed that HAP in particular, but also TP and BF, can reflect MVD, similar to the findings of previous reports. There was no significant correlation between MVD and HPI, similar to the report by Yang et al. (24), but different from the findings of Jiang et al. (25); we speculate that the cause of this may be related to immature angiogenesis and micro-arteriovenous fistula formation with contrast agent extravasation. Even so, HPI still shows that blood supply of VX2 tumor mainly comes from hepatic artery (60%–65%), being significantly higher than normal hepatic parenchyma(24%–29%). In our opinion, HAP, HPI, and BF are sensitive indicators to reflect arterialization of neovascularization and MVD in the tumor. BV cannot reflect MVD, similar to findings of a previous report (25). Its exact mechanism may be associated with: 1) immature neoangiogenesis with potential abnormal shunts and increased permeability, resulting in contrast agent exosmosis; 2) in theory, BV equals BF multiplied by average transmit time, but it is affected by the maturity of neoangiogenesis and the degree of openness and abnormal communication of the neovasculature, which is regulated by multiple growth factors; 3) the influence of hepatic dual blood supply. In a word, the relationship between BV and neovascularization cannot be fully explained and still needs further study.

Our study has several limitations: 1) CTPI was performed under deep anesthesia with free breathing, and respiratory motion artifact may influence the accuracy of the data; 2) the maximum slope model adopted in this study cannot calculate mean transmission time and hepatic permeability of capillary vessel surface; 3) bias of MVD calculated by histopathology; 4) small animal models adopted in our study may affect the accuracy of data due to relatively higher scanning parameters, which would not decrease image quality tremendously. We did not investigate how far CT radiation exposure parameters could be reduced without impairing the CTPI parameters, which needs further research in the future. In addition, rabbit VX2 tumor is different from primary hepatic carcinoma with cirrhosis background and the change of microvessels are different, which may result in some difference of perfusion parameters between animal models and humans; 5) the animal sample size was small; 6) the subjective image quality was not analyzed because we especially focused on objective parameters; and 7) IR was not implemented in the data acquisition in our study, which might even increase the potential of IR.

In conclusion, it is feasible to perform CTPI with low radiation dose and improve image quality using newer reconstruction algorithms. CTPI parameters are not affected by tube voltage, tube current, or reconstruction algorithms, and HAP can best reflect MVD, but no correlation exists between BV and MVD. Therefore, we expect hepatic CTPI with low radiation dose to be used more frequently in future for evaluation of perfusion, as it will be useful to reduce patients' concern about radiation exposure and is more valuable for differential diagnosis and monitoring treatment response of hepatic tumors.

Conflict of interest disclosure

The authors declared no conflicts of interest.

References

1. Bray F, Ferlay J, Soerjomataram I, et al. Global cancer statistics 2018: GLOBOCAN estimates of incidence and mortality worldwide for 36 cancers in 185 countries. CA Cancer J Clin 2018; 68: 394–424. [Crossref]
2. Omata M, Cheng AL, Kokudo N, et al. Asia-Pacific clinical practice guidelines on the management of hepatocellular carcinoma: a 2017 update. Hepatol Int 2017; 11:317–370. [Crossref]

3. Eisenhauer EA, Therasse P, Bogaerts J, et al. New response evaluation criteria in solid tumours: revised RECIST guideline (version 1.1). Eur J Cancer 2009; 45:228–247. [Crossref]
4. Lencioni R, Llovet JM. Modified RECIST (mRECIST) assessment for hepatocellular carcinoma. Semin Liver Dis 2010; 30:52–60. [Crossref]
5. Materne R, Smith AM, Peeters F, et al. Assessment of hepatic perfusion parameters with dynamic MRI. Magn Reson Med 2002; 47:135–142. [Crossref]
6. Goetti R, Reiner CS, Knuth A, et al. Quantitative perfusion analysis of malignant liver tumors: dynamic computed tomography and contrast-enhanced ultrasound. Invest Radiol 2012; 47:18–24. [Crossref]
7. Reiner CS, Goetti R, Burger IA, et al. Liver perfusion imaging in patients with primary and metastatic liver malignancy: prospective comparison between 99mTc-MAA spect and dynamic CT perfusion. Acad Radiol 2012; 19:613–621. [Crossref]
8. Ren Y, Fleischmann D, Foygel K, et al. Antiangiogenic and radiation therapy: early effects on in vivo computed tomography perfusion parameters in human colon cancer xenografts in mice. Invest Radiol 2012; 47:25–32. [Crossref]
9. Ash L, Teknos TN, Gandhi D, et al. Head and neck squamous cell carcinoma: CT perfusion can help noninvasively predict intratumoral microvessel density. Radiology 2009; 251:422–428. [Crossref]
10. Goh V, Halligan S, Daley F, et al. Colorectal tumor vascularity: quantitative assessment with multidetector CT--do tumor perfusion measurements reflect angiogenesis? Radiology 2008; 249:510–517. [Crossref]
11. Kim JW, Jeong YY, Chang NK, et al. Perfusion CT in colorectal cancer: comparison of perfusion parameters with tumor grade and microvessel density. Korean J Radiol 2012; 13 Suppl 1:S89–97. [Crossref]
12. Kim DH, Kim SH, Im SA, et al. Intermodality comparison between 3D perfusion CT and 18F-FDG PET/CT imaging for predicting early tumor response in patients with liver metastasis after chemotherapy: preliminary results of a prospective study. Eur J Radiol 2012; 81:3542–3550. [Crossref]
13. Kim SH, Kamaya A, Willmann JK. CT perfusion of the liver: principles and applications in oncology. Radiology 2014; 272:322–344. [Crossref]
14. Liang C. Pay attention to the relative radiation of CT. Zhonghua Yi Xue Za Zhi 2014; 94:3361–3362.
15. Kalra MK, Maher MM, Toth TL, et al. Strategies for CT radiation dose optimization. Radiology 2004; 230:619–628. [Crossref]
16. Li JL, Huang MP, Cao XM, et al. Individualized reduction of radiation dose with a chest circumference-adapted technique and iterative reconstructions in 256-slice retrospective and prospective ECG-triggered computed tomography coronary angiography. Coron Artery Dis 2015; 26:308–316. [Crossref]
17. Mello-Amoedo CD, Martins AN, Tachibana A, et al. Comparison of radiation dose and image quality of abdominopelvic CT using iterative (AIDR 3D) and conventional reconstructions. AJR Am J Roentgenol 2018; 210:127–133. [Crossref]
18. Mileto A, Zamora DA, Alessio AM, et al. CT detectability of small low-contrast hypoattenuating focal lesions: iterative reconstructions versus filtered back projection. Radiology 2018; 289:443–454. [Crossref]
19. Mitsumori LM, Shuman WP, Busey JM, et al. Adaptive statistical iterative reconstruction versus filtered back projection in the same patient: 64 channel liver CT image quality and patient radiation dose. Eur Radiol 2012; 22:138–143. [Crossref]
20. Willemink MJ, Leiner T, de Jong PA, et al. Iterative reconstruction techniques for computed tomography part 2: initial results in dose reduction and image quality. Eur Radiol 2013; 23:1632–1642. [Crossref]
21. Anzidei M, Napoli A, Zaccagna F, et al. Liver metastases from colorectal cancer treated with conventional and antiangiogenetic chemotherapy: evaluation with liver computed tomography perfusion and magnetic resonance diffusion-weighted imaging. J Comput Assist Tomogr 2011; 35:690–696. [Crossref]
22. Negi N, Yoshikawa T, Ohno Y, et al. Hepatic CT perfusion measurements: a feasibility study for radiation dose reduction using new image reconstruction method. Eur J Radiol 2012; 81:3048–3054. [Crossref]
23. Zhang CY, Cui YF, Guo C, et al. Low contrast medium and radiation dose for hepatic computed tomography perfusion of rabbit VX2 tumor. World J Gastroenterol 2015; 21:5259–5270. [Crossref]
24. Yang HF, Du Y, Ni JX, et al. Perfusion computed tomography evaluation of angiogenesis in liver cancer. Eur Radiol 2010; 20:1424–1430. [Crossref]
25. Jiang HJ, Zhang ZR, Shen BZ, et al. Quantification of angiogenesis by CT perfusion imaging in liver tumor of rabbit. Hepatobil Pancreat Dis Int 2009; 8:168–173.